Impact of Oxygen on Photopolymerization Kinetics and Polymer Structure

Allison K. O'Brien[†] and Christopher N. Bowman*[,†,‡]

Department of Chemical Engineering, University of Colorado, Boulder, Colorado 80309-0424, and Department of Restorative Dentistry, University of Colorado Health Sciences Center, Denver, Colorado 80045-0508

Received August 24, 2005; Revised Manuscript Received January 29, 2006

ABSTRACT: The effects of varying polymerization conditions on the extent of oxygen inhibition of free-radical photopolymerization were investigated using both experimental and modeling efforts. Specifically, sample thickness, initiation rate, and oxygen concentration were varied, and the resulting photopolymerization kinetics were studied using real-time FTIR and a comprehensive photopolymerization model. As the sample thickness was increased, the overall average double-bond conversion increased due to the greater conversion in the lower depths of the films. Because of the dramatic inhibition at the top of the film, this led to heterogeneity in the film's conversion as shown with the comprehensive model. Increasing the initiation rate decreased the inhibition time and increased the overall average double-bond conversion due to an increase in the overall radical production, allowing better competition of the propagation reaction with the inhibition reaction. The oxygen concentration was varied, and as the oxygen concentration increased, the overall inhibition reaction increased, thus lowering the overall double-bond conversion. Finally, the effect of oxygen concentration on the bulk mechanical properties of the film was determined. It was found that no statistical difference was observed in the mechanical properties for films exposed to argon ($P_{O_2} = 0$) as compared to a film exposed to air ($P_{O_2} = 0.21$).

Introduction

Photopolymerization of multivinyl monomers is a widely accepted and growing process.[1−3] Countless products are produced utilizing photopolymerization including paints, coatings, adhesives, inks, microelectronics, optical materials, dental resins, and, more recently, three-dimensional stereolithography and holographic recordings.[1−7] The extensive uses and applications of photoinitiated polymerization are due to its many advantages over other polymerization processes including that they are rapid, have reduced energy requirements, readily occur at room temperature, and are low cost.[2,3,8,9] Another benefit is that these polymerizations are spatially and temporally controllable since the initiating light is resolvable in both space and time.[7] Additionally, the initiation rate is independently dictated by the choice of photoinitiator (i.e., its molar absorption coefficient, quantum yield, and efficiency) and the light intensity. An environmental benefit of photopolymerizations is that the monomer is often polymerized in bulk, eliminating the need for environmentally hazardous solvents. Finally, if multivinyl monomers are used, then cross-linking of the resulting polymer occurs, imparting unique physical properties to the product.[5] Unfortunately, despite all of these benefits, there still exist many limitations, including oxygen inhibition and attenuated penetration of the light source into the sample.[10−21]

The goal of this study was to improve the understanding of the inhibitory effect of oxygen on the photopolymerization of multifunctional monomers. Free radical photopolymerization transforms a multifunctional monomer into a cross-linked macromolecule by a chain reaction initiated by reactive species.[1] The initiating reactive speciesis formed by a photoinitiator absorbing the incident light and photocleaving into initiating radicals. The initiating radicals combine with available monomer, forming primary radicals that subsequently propagate through additional monomer units to create a three-dimensional polymer network.[1,8,22,23] Unfortunately, molecular oxygen inhibits several steps in this reaction pathway, reducing the overall effectiveness of the polymerization or requiring expensive and impractical initiation strategies.

Molecular oxygen is known to inhibit free radical polymerizations by reacting with initiator, primary, and growing polymer radicals to form peroxy radicals.[16−18,24,25] The peroxy radicals are more stable and do not readily reinitiate polymerization, and thus, the oxygen essentially terminates or consumes radicals.[7] If oxygen is present, an induction time will be observed since the polymerization cannot proceed until the propagation reaction competes with the inhibition reaction.[7] As the equilibrium dissolved oxygen concentration in acrylates is $\sim 10^{-3}$ M[18,26] and Decker et al. report that the oxygen concentration below which polymerization proceeds is $\sim 4 \times 10^{-6}$ M, the oxygen concentration must drop by a factor of at least 300 before polymerization begins. At high concentrations or in very thin films, oxygen scavenges all of the radicals in the polymerization and thus inhibits or severely retards the polymerization. In thin films oxygen inhibition is more important as oxygen readily diffuses back into the sample from the surroundings. In thicker films the lower depths of the film polymerize, while the top layer remains "tacky" as the oxygen inhibits the surface reaction. The unpolymerized top layer reduces surface and optical properties.[18,27]

Several techniques have been utilized to combat the effects of oxygen inhibition. The use of high-intensity irradiation sources increases the initiation rate by increasing the production of primary radicals such that it becomes much greater than their consumption by oxygen. Another alternative is to polymerize the samples in an inert environment, whereby the oxygen is eliminated from the polymerization.[18,25,28,29] There are also several methods that include the addition of molecules to reduce

[†] University of Colorado.
[‡] University of Colorado Health Sciences Center.
* To whom correspondence should be addressed: Fax 303-492-4341; e-mail bowmanc@colorado.edu.

10.1021/ma051863l CCC: $33.50
Published on Web 03/03/2006

the inhibitory effect of oxygen. Decker developed a method whereby the dissolved oxygen in a monomer system was consumed prior to and during polymerization using a dual-initiation method with the addition of an oxygen singlet generator and acceptor molecule.[16,17] Furthermore, the addition of thiols and amines to monomer systems is known to decrease the deleterious effects of oxygen.[25,30−32]

Because of the immense interest in and importance of the photopolymerization process, it is of great value to understand fully the impact of oxygen on photopolymerization as a means to combat its inhibitory effects. Past research has documented the effect of oxygen, primarily focusing on the polymerization rate reduction.[6,20,27,33,34] Nunes et al. utilized spatially resolved MRI to investigate the anisotropic effects of oxygen on the photopolymerization of dental materials.[35,36] Additionally, Chong et al.[21] and Krongauz et al.[20] developed early kinetic models that simulated specific effects oxygen had on photopolymerization kinetics. Recently, Dickey et al.[37] developed a quasi-steady-state approximation kinetic model to study the effect of diffusing oxygen at the etch barrier in step and flash imprint lithography. However, an extensive, in-depth study has not been conducted into the impact of oxygen on photopolymerization kinetics and the resulting polymer structure. Thus, in this study, a better understanding of the inhibitory effect of oxygen will be obtained through systematic experimental probing and comparison of experimental results with simulation prediction.

Specifically, we have studied several key factors that affect the extent of oxygen inhibition in photopolymerization kinetics. The effects of sample thickness, ambient oxygen concentration, and initiation rate have been investigated and modeled. Furthermore, the effect of dissolved oxygen on the bulk mechanical properties has been widely hypothesized. It has been noted that the cross-link density and the shear modulus of the polymer are lower.[25] However, this has yet to be experimentally investigated, and thus, in this paper we look into the effect on the initial dissolved oxygen concentration on the resulting bulk polymer properties. Finally, a 1-D comprehensive kinetic photopolymerization model is applied to simulate experimental conditions and proves to be a useful tool in predicting photopolymerization kinetic behavior.

Experimental Section

Materials. The monomer used in this investigation was 1,6-hexanediol diacrylate (HDDA) (Aldrich, Milwaukee, WI), as it is well characterized and exhibits the appropriate cure kinetics required for this study (chain length independent termination and rapid polymerization rate). The polymerizations were performed with the initiator 2,2-dimethoxy-2-phenylacetophenone (DMPA, Ciba Geigy, Hawthorne, NY). The surfactant BYK 307, a polyether modified dimethylpolysiloxane copolymer (BYK-Chemie, Wesel, Germany), was utilized at 0.01 wt % to provide more uniform surface characteristics in the nonlaminated films and minimizes the change in film thickness. For the oxygen concentration determination procedure, dimethylanthracene (DMAC) and 5,10,15,20-tetraphenyl-21*H*,23*H*-porphine zinc (ZnTPP) were used (Aldrich, Milwaukee, WI). All materials were used as received.

Methods. Fourier transform infrared (FTIR) spectroscopy (Nicolet model 760 Magna Series II FTIR, Nicolet, Madison, WI) was used to obtain extents of polymerization and to examine the polymerization kinetics of the monomer systems studied. A horizontal transmission apparatus (HTA) accessory was used to enable mounting of the samples in a horizontal orientation for FTIR measurements.[38] The HTA has a controlled polymerization atmosphere, thus allowing the samples to be exposed to controlled, varying concentrations of oxygen in an oxygen/nitrogen mixture. The double-bond conversion was determined from the change in absorbance of the acrylate [C═C] double-bond peak. FTIR measures the average absorbance through the depth of a sample; thus, an average conversion was determined using this method. In the mid-IR range the acrylate peak was at 1604−1648 cm^{-1}, and in the near-IR range the peak was at 6207−6122 cm^{-1}. Monomer samples were placed on NaCl crystals and rolled to a uniform thickness using wire-wound rods (Gardco, Pompano Beach, FL), placed in the HTA, and allowed to equilibrate with the ambient environment for 15 min. The polymerization reaction was initiated using a UV light source (Ultracure 100SS 100 W HG short-arc lamp, EXFO, Mississaugua, Ontario, Canada) equipped with a liquid light guide (8 mm, EXFO, Mississaugua, Ontario, Canada) and filter (320−500 nm). Irradiation intensities were measured with an International Light, Inc., model IL1400A radiometer (Newburyport, MA).

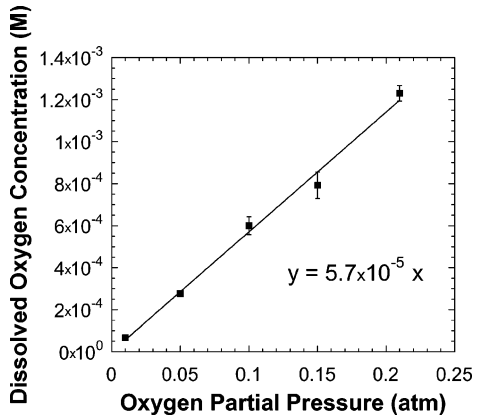

Figure 1. Equilibrium dissolved oxygen concentration in 1,6-hexanediol diacrylate when exposed to various partial pressures of oxygen.

Dynamic mechanical analysis (DMA) (Perkin-Elmer DMA7e, Norwalk, CT) was performed to investigate the glass transition temperature and storage modulus in our polymer systems. Monomer samples for DMA analysis were bubbled with argon, 1%, 5%, 10%, or 21% oxygen for 15 min, and then immediately polymerized with 1 mW/cm^2, while monitoring the conversion with near-IR spectroscopy, to 85 ± 2% double-bond conversion. The polymer samples were of uniform size (13.5 × 2.5 × 0.9 mm^3). DMA was performed over a temperature range of −30 to 150 °C, with a ramping rate of 5 °C/min using extension mode (sinusoidal stress of 1 Hz frequency). The loss tangent (tan δ, the ratio of loss to storage modulus) and storage modulus were recorded as a function of temperature. The glass transition temperature, T_g, was taken to be the maximum of the loss tangent vs temperature curve.

Ultraviolet−visible spectroscopy (UV−vis) was used to obtain the extent of consumption of dimethylanthracene to determine the equilibrium oxygen concentration in the monomer. This method has been previously described by Gou et al.[26] The excitation source used was a Dolan-Jenner DC-950 dc-regulated fiber-optic illuminator (Lawrence, MA) with a red filter. The UV−vis spectrometer (Perkin-Elmer Lambda 40 UV/vis systems, Perkin-Elmer, Shelton, CT) monitored the DMAC absorption at 380 nm during the reaction of singlet oxygen and DMAC to form a complex. The monomer was equilibrated with various oxygen partial pressures, and the resulting equilibrium oxygen concentration was determined as shown in Figure 1.

The film thickness was calibrated by sandwiching plastic shims of known thickness (Small Parts, Inc., Miami Lakes, FL) between two NaCl crystals and then wicking in the monomer of interest. The [C═C] peak area was measured using FTIR spectroscopy, and the area was correlated to the shim thickness.

An unsteady-state one-dimensional kinetic photopolymerization model that allows for variation of temperature, species concentration, and light intensity throughout the thickness of the polymerization film was previously developed.[15,19,39,40] Heat transfer effects are important as the kinetic constants, and the diffusion coefficients are functions of temperature. Diffusion of small species (such as

Table 1. Parameters Used in the Comprehensive Kinetic Model Are Listed along with Reference from Which the Value Was Obtained[a]

parameter	description	value	units	reference
k_{p0}	propagation constant	5.0×10^8	L/(mol s)	Goodner et al.[41]
k_{t0}	termination constant	7.0×10^{14}	L/(mol s)	Goodner et al.[41]
$D_{I,0}$	initiator diffusion preexponential factor	3.93×10^{14}	cm^2/s	Wilke−Change equation
$D_{M,0}$	monomer diffusion preexponential factor	2.61×10^{14}	cm^2/s	Wilke−Change equation
$D_{z,0}$	oxygen diffusion preexponential factor	4.80×10^{14}	cm^2/s	Wilke−Change equation
MW_M	monomer molecular weight	226.28	g/mol	Aldrich
ρ_M	monomer density	1.01	g/mL	Aldrich
$[M]_0$	monomer initial concentration	8.92	mol/L	calculated
T_{gm}	glass transition temperature of monomer	278	K	Goodner et al.[41]
T_{gp}	glass transition temperature of polymer	350	K	Goodner et al.[41]

[a] The monomer values refer to 1,6-hexanediol diacrylate (HDDA), and initiator values are for 2,2-dimethoxy-2-phenylacetophenone.

initiator, monomer, primary radical, and oxygen molecules) is an important aspect of photopolymerizations, and thus, mass transfer is also critical. The model is based on the classical mechanisms for free radical photopolymerization. This includes initiation (from the photolysis of the initiator), propagation, and termination as well as oxygen inhibition kinetics. The kinetic constants used in this work incorporate Arrhenius temperature dependence, diffusion-controlled kinetics, and termination by reaction diffusion. The latter two phenomena are described in terms of fractional free volume of the polymerizing mixture.

Several assumptions are incorporated into the model. Summarized, they are (i) the light source is monochromatic at 365 nm, and the initiation reaction is assumed to generate two primary radicals of equal reactivity and mobility; (ii) to simulate the polymerization in a thick sample, the sample is divided into uniform slices over which the light intensity, species concentration, and temperature are constant within the slice; (iii) the volume of each of these slices is assumed to be constant over the course of the reaction; (iv) propagation, termination, and inhibition are assumed to be chain length independent; (v) bimolecular termination is characterized by a lumped k_t that accounts for both combination and disproportionation; and (vi) physical and thermal properties of the system (density, specific heat, and conductivity) are assumed to remain constant throughout the course of the reaction.

The model was applied in this study to investigate further experimental systems using the experimental parameters and environmental conditions in the simulation. The parameters used in the model were for the monomer 1,6-hexanediol diacrylate and initiator 2,2-dimethoxy-2-phenylacetophenone. All parameters used are described in Goodner et al.,[39] except those noted in Table 1.

Results and Discussion

The extent of oxygen inhibition during free-radical photopolymerization is affected by many variables, including film thickness, dissolved oxygen concentration, and initiation rate. The film thickness affects oxygen inhibition in that there is a competition between the diffusion of oxygen into the film and the polymerization reaction, which increases viscosity and eventually reduces the oxygen diffusion coefficient significantly. Thus, the greater the distance the oxygen molecule must diffuse, the higher the likelihood that the polymerization reaction will occur. Similarly, the thinner the film, the more readily oxygen diffuses throughout the whole film, consuming all radicals present and completely inhibiting the reaction. The characteristic diffusion time for oxygen is described by the quantity $(L/2)^2/D$, or half of the characteristic diffusion length squared divided by the diffusion coefficient. Thus, a 10 μm sample has a characteristic diffusion time on the order of 0.25 s, while a 100 μm sample has a characteristic time on the order of 25 s (assuming oxygen has a diffusivity of $\sim 10^{-6}$ cm^2/s in HDDA). In this manner, it can be seen that the film thickness plays an important role in determining the extent of oxygen inhibition as well as a role in the heterogeneity of the film's properties.

Figures 2 and 3 show the effect film thickness has on the extent of oxygen inhibition with both experimental and modeling results. As film thickness increases, the average polymerization rate also increases, as does the average double-bond conversion, as shown in Figure 3. We can further look at the effect of film thickness, noting the trend that as film thickness increases, the conversion increases up to a critical thickness of about 200 μm, where the majority of the film has polymerized, as shown in Figure 2. It is important to note that the conversion values shown in Figures 2 and 3 are values averaged for the whole film. This overshadows the great heterogeneity that exists within the films. The model simulations in both Figures 2 and 3 overall match the experimental data very well, with the exception of the autoacceleration regime. Future work will be conducted toward refining the parameters that define this region. Figure 4 shows the simulated depth profile for the 45 μm sample, which details the great difference in double-bond conversion throughout the film. The top 10 μm of the films have minimal conversion, while the lower depths of the film have almost complete conversion. This difference causes a tacky layer to form on the top of the film, while the rest of the film is well-cured, vitrified, and hard.

Another variable that dramatically affects the extent of oxygen inhibition of free-radical photopolymerizations is the initiation

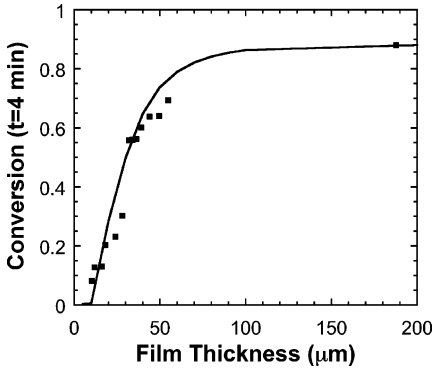

Figure 2. Double-bond conversion at a cure time of 4 min vs film thickness. $P_{O_2} = 0.21$ atm. DMPA = 0.1 M (2.5 wt %), light intensity = 30 mW/cm^2.

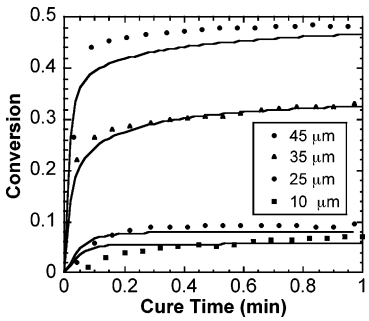

Figure 3. Double-bond conversion vs cure time for samples with varying thickness. $P_{O_2} = 0.21$ atm. DMPA = 0.2 M (5 wt %), light intensity = 50 mW/cm^2. Model simulations are shown with lines.

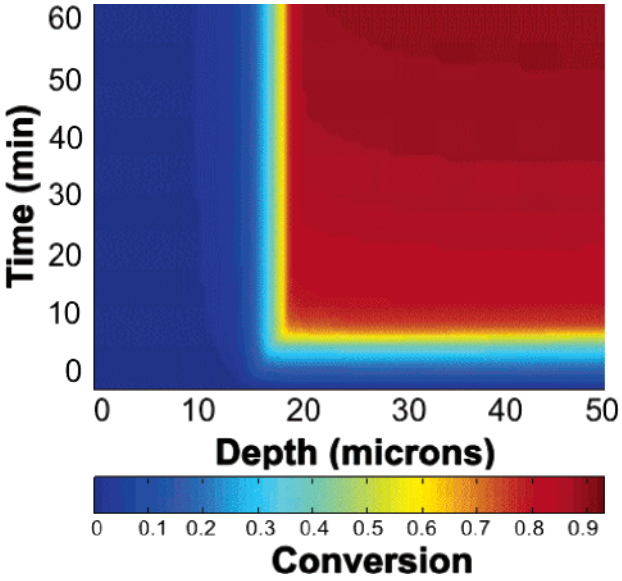

Figure 4. Model simulations of double-bond conversion as a function of cure time and sample depth. $P_{O_2} = 0.21$ atm. DMPA = 0.2 M (5 wt %), light intensity = 50 mW/cm^2.

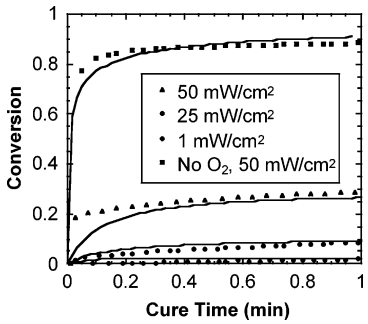

Figure 5. Double-bond conversion vs cure time for samples with varying irradiating light intensities. $P_{O_2} = 0.1$ atm DMPA = 0.2 M (5 wt %), thickness = 12 μm. Model simulations are shown with lines.

rate. Polymerization will not occur until it competes with the inhibition reaction. Because of the fact that the inhibition rate constant is 4 orders of magnitude greater than the propagation rate constant, and the equilibrium oxygen concentration of acrylates in air is $\sim 10^{-3}$ M, nearly all of the oxygen must be consumed for the polymerization rate to be significantly greater than the inhibition rate.[5,18] Thus, if this point is reached very rapidly, the polymerization that occurs will increase the film's viscosity and decrease oxygen's ability to diffuse, and there will be ample initiator remaining to facilitate near complete double-bond conversion to occur. Conversely, if this condition is reached very slowly, a large quantity of the initiator will be consumed in the process, and very little polymerization will occur due to the limited remaining initiator. Figure 5 shows the effect of varying the irradiating light intensity on oxygen inhibition of free-radical photopolymerizations. The initiation rate is defined as[22]

$$R_i = \phi \epsilon I C_I \tag{1}$$

where ϕ is the initiator efficiency, ϵ is the initiator molar absorptivity, C_I is the initiator concentration, and I is the light intensity. Thus, as the light intensity is increased, the initiation rate proportionally increases. As the light intensity increases, the photopolymerization reaction will be able to better compete with the inhibition reaction. In Figure 5, the film irradiated with 1 mW/cm^2 has very low double-bond conversion, yet as the

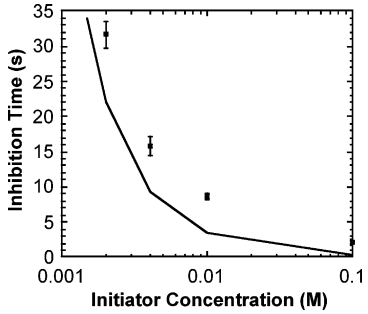

Figure 6. Inhibition time vs initiator concentration of HDDA equilibrated in air and then laminated. Light intensity = 5 mW/cm^2, sample thickness = 50 μm. Model simulations are shown with lines.

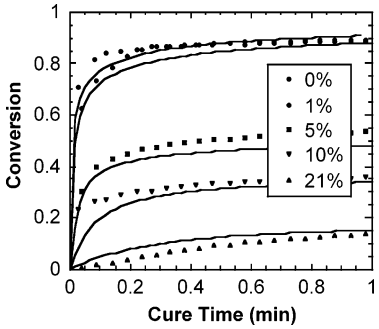

Figure 7. Double-bond conversion vs cure time for samples exposed to varying oxygen concentrations. Light intensity = 50 mW/cm^2, DMPA = 0.2 M (5 wt %), thickness = 12 μm. Model simulations are shown with lines.

light intensity is increased to 25 and then 50 mW/cm^2, the polymerization rate and double-bond conversion both increase. However, a light intensity much greater than 50 mW/cm^2 is required to achieve as high a conversion as the film with no oxygen present. We can look further at the relationship between the initiation rate and oxygen inhibition in Figure 6. The inhibition time for the polymerization reaction is the time it takes for an inhibitor, oxygen, to be removed from the system, and the polymerization reaction to start. This time approximated as follows:

$$t_{inhib} \approx \frac{[O_2]_{cons}}{R_i} \tag{2}$$

where $[O_2]_{cons}$ is the amount of oxygen that needs to be consumed and R_i is the initiation rate. It has previously been found that the $[O_2]_{ss}$, the steady-state oxygen concentration in the film, is on the order of 10^{-6} M,[5,18] and thus with the equilibrium oxygen concentration in acrylates at $\sim 10^{-3}$ M, nearly all of the oxygen must be consumed for the reaction to proceed. From eq 2, it is seen that as the initiation rate is increased, the inhibition time decreases, as also confirmed by Figure 6.

Finally, the effect of the ambient oxygen concentration on oxygen inhibition was explored. The dissolved oxygen concentration in the monomer is affected by both the partial pressure of oxygen surrounding the monomer film and the chemistry of the monomer itself. Thus, by varying the ambient partial pressure of oxygen, the dissolved oxygen concentration will change and dramatically affect the oxygen diffusion rate and the extent of inhibition of the polymerization. Figure 7 shows the effect that increasing the oxygen diffusion rate by increasing the ambient oxygen concentration has on the polymerization reaction kinetics. As the ambient oxygen concentration is increased, the dissolved oxygen concentration at the monomer film's surface

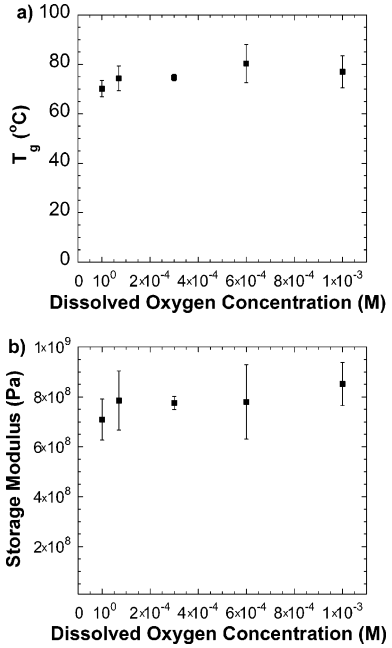

Figure 8. Glass transition temperature (a) and storage modulus (b) at 25 °C of HDDA with varying initial dissolved oxygen concentrations from argon (0 atm) to air (0.21 atm). All samples were cured with a light intensity of 1 mW/cm^2 and 0.1 wt % DMPA to a final double-bond conversion of 85 ± 2%. Sample dimensions were 13.5 × 2.5 × 0.9 mm^3.

will increase, and the subsequent oxygen diffusion rate into the film will also increase. The increase in the diffusion rate will allow the oxygen inhibition reaction to compete with the polymerization reaction, causing greater inhibition of the polymerization reaction, as shown in Figure 7.

It is well-known that the diffusion of oxygen into the monomer film and subsequent inhibition of the photopolymerization reaction at the very top of the film cause a liquid, tacky layer to remain on top of the polymerized film. However, the effect of the dissolved oxygen on the bulk mechanical properties of the polymerized film has not previously been quantified systematically. It has been suggested by Krongauz et al.[25] that the peroxy radicals formed when oxygen is present cause a higher termination rate that leads to lower cross-link densities and lower shear modulus. When the film is open to air, very little polymerization is achieved, especially at the top of the film; thus, the lower overall conversion greatly reduces the mechanical properties and has a greater effect than the quantity of short chains due to the terminating peroxy radicals. Thus, it was of interest to investigate how the short chains affected laminate films that had distinctly different dissolved oxygen concentrations. Films of HDDA were exposed to varying initial oxygen concentrations, then laminated, and polymerized to the same double-bond conversion. The glass transition temperature and shear modulus of these films are shown in Figure 8. It can be seen that as the initial dissolved oxygen concentration was varied in the films, there is a negligible effect on the bulk mechanical properties. When compared to the oxygen concentration of HDDA in air, the initial monomer concentration is almost 5 orders of magnitude greater, and the polymer radical concentration is about 1 order of magnitude greater (as determined by model simulations); thus, the concentration of short chains formed if all the oxygen forms peroxy radicals will be very minimal. These relative amounts imply that the short chains have a negligible plasticizing effect. Therefore, oxygen has very little effect on bulk mechanical properties. However, the heterogeneity of double-bond conversion in films polymerized in samples open to air will reduce mechanical properties and may lead to undesirable products.

Conclusions

The impact of oxygen on the photopolymerization of HDDA was investigated using both experimental and modeling efforts. Specifically, the effects of varying film thickness, light intensity, and oxygen concentration on the extent of oxygen inhibition of the polymerization reaction were studied. As the film thickness was increased, the overall average conversion in the film increased due to the lack of oxygen diffusion to the lower depths of the film. However, simulations showed that there was great heterogeneity in the double-bond conversion profile due to the complete inhibition of the reaction in the top 10 μm of the film. Increasing light intensity or the initiation rate increased the rate of radical production, allowing the polymerization reaction to occur before oxygen diffused back into the film. This polymerization in turn increased the double-bond conversion and increased the viscosity significantly, blocking oxygen diffusion completely. Finally, the effect of the initial dissolved oxygen concentration on the resulting bulk mechanical properties was examined. It was found the due to the low concentration of short chains formed from the peroxy radicals, no plasticizing effect was observed in these films.

Acknowledgment. This work was supported through grants from the Industry/University Cooperative Research Center (I/UCRC) for the Fundamentals and Application of Photopolymerizations and the National Institute of Health (DE10959). In addition, we thank the Department of Education's Graduate Assistance in Areas of National Need (GAANN) program for a fellowship awarded to A.K.O.

References and Notes

(1) Decker, C. *Acta Polym.* **1994**, *45*, 333−347.
(2) Decker, C. *Macromol. Rapid Commun.* **2002**, *23*, 1067−1093.
(3) Andrzejewska, E. *Prog. Polym. Sci.* **2001**, *26*, 605−665.
(4) Decker, C.; Moussa, K. *J. Coat. Technol.* **1993**, *65*, 49−57.
(5) Selli, E.; Bellobono, I. R. *Photopolymerization of Multifunctional Monomers: Kinetic Aspects*; Chapman and Hall: London, 1993; Vol. III, pp 1−32.
(6) Decker, C.; Moussa, K. *Makromol. Chem., Macromol. Chem. Phys.* **1988**, *189*, 2381−2394.
(7) Kloosterboer, J. G. Network Formation by Chain Crosslinking Photopolymerization and its Applications in Electronics. *Adv. Polym. Sci.* **1988**, *84*, 1−61.
(8) Decker, C. *J. Coat. Technol.* **1987**, *59*, 97−106.
(9) Decker, C. New Developments in UV-Curable Acrylic Monomers. *Radiat. Curing Polym. Sci. Technol.* **1993**, *3*, 33−63.
(10) Terrones, G.; Pearlstein, A. J. *Macromolecules* **2001**, *34*, 8894−8906.
(11) Terrones, G.; Pearlstein, A. J. *Macromolecules* **2001**, *34*, 3195−3204.
(12) Miller, G. A.; Gou, L.; Narayanan, V.; Scranton, A. B. *J. Polym. Sci., Part A: Polym. Chem.* **2002**, *40*, 793−808.
(13) Ivanov, V. V.; Decker, C. *Polym. Int.* **2001**, *50*, 113−118.
(14) Guthrie, J.; Jeganathan, M. B.; Otterburn, M. S.; Woods, J. *Polym. Bull. (Berlin)* **1986**, *15*, 51−58.
(15) O'Brien, A. K.; Bowman, C. N. *Macromolecules* **2003**, *36*, 7777−7782.
(16) Decker, C. *Makromol. Chem., Macromol. Chem. Phys.* **1979**, *180*, 2027−2030.
(17) Decker, C.; Faure, J.; Fizet, M.; Rychla, L. *Photogr. Sci. Eng.* **1979**, *23*, 137−140.
(18) Decker, C.; Jenkins, A. D. *Macromolecules* **1985**, *18*, 1241−1244.
(19) Lovestead, T. M.; O'Brien, A. K.; Bowman, C. N. *J. Photochem. Photobiol., A* **2003**, *159*, 135−143.
(20) Krongauz, V. V.; Schmelzer, E. R. *Polymer* **1992**, *33*, 1893−1901.
(21) Chong, J. S. *J. Appl. Polym. Sci.* **1969**, *13*, 241−247.
(22) Odian, G. *Principles of Polymerization;* John Wiley & Sons: New York, 1991; p 768.
(23) Fouassier, J. P.; Rabek, J. F. *Radiation Curing in Polymer Science and Technology*; Elsevier Science Publishing, Ltd.: Essex, England, 1993; Vol. 1.

(24) Miller, C. W.; Hoyler, C. E.; Jonssen, S.; Nason, C.; Lee, T. Y.; Kuang, W. F.; Viswanathan, K. *N-Vinylamides and Reduction of Oxygen Inhibition in Photopolymerization of Simple Acrylate Formulations*, 1st ed.; American Chemical Society: Washington, DC, 2003; p 1.
(25) Krongauz, V. V.; Chawla, C. P.; Dupre, J. *Oxygen and Radical Photopolymerization in Film*, 1st ed.; American Chemical Society: Washington, DC, 2003; p 1.
(26) Gou, L.; Corestsopoulous, N.; Scranton, A. B. *J. Polym. Sci., Part A: Polym. Chem.* **2003**, *42*, 1285−1292.
(27) Cao, H.; Currie, E.; Tilley, M.; Jean, Y. C. Oxygen Inhibition Effect on Surface Properties of UV−Curable Acrylate Coatings. In *Photoinitiated Polymerization*; Belfield, K. D., Crivello, J. V., Eds.; 2003.
(28) Studer, K.; Decker, C.; Beck, E.; Schwalm, R. *Prog. Org. Coat.* **2003**, *48*, 92−100.
(29) Studer, K.; Decker, C.; Beck, E.; Schwalm, R. *Prog. Org. Coat.* **2003**, *48*, 101−111.
(30) Davidson, R. S. *The Role of Amines in UV Curing*; Chapman and Hall: London, 1993; Vol. III.
(31) Lecamp, L.; Houllier, F.; Youssef, B.; Bunel, C. *Polymer* **2001**, *42*, 2727−2736.
(32) Cramer, N. B.; Bowman, C. N. *J. Polym. Sci., Part A: Polym. Chem.* **2001**, *39*, 3311−3319.
(33) Decker, C. *Macromolecules* **1989**, *22*, 12.
(34) Decker, C.; Moussa, K. *Makromol. Chem., Macromol. Chem. Phys.* **1990**, *191*, 963−979.
(35) Nunes, T. G.; Ceballos, L.; Osorio, R.; Toledano, M. *Biomaterials* **2005**, *26*, 1809−1817.
(36) Pereira, S. G.; Reis, N.; Nunes, T. G. *Polymer* **2005**, *46*, 8034−8044.
(37) Dickey, M. D.; Burns, R. L.; Kim, E. K.; Johnson, S. C.; Stacey, N. A.; Willson, C. G. *AIChE J.* **2005**, *51*, 2547−2555.
(38) Berchtold, K. A.; Bowman, C. N. In RadTech Europe '99, Berlin, Germany, 1999; p 767.
(39) Goodner, M. D.; Bowman, C. N. *Chem. Eng. Sci.* **2002**, *57*, 887−900.
(40) O'Brien, A. K.; Bowman, C. N. *Macromol. Theory Simul.* **2006**, *15*, 176−182.
(41) Goodner, M. D.; Lee, H. R.; Bowman, C. N. *Ind. Eng. Chem. Res.* **1997**, *36*, 1247−1252.

MA051863L